

1 In Silico Determination of *Tinospora cordifolia* Phytochemicals as Potential DPP-4 Inhibitors for Type 2 Diabetes
2 Management

3
4 Ebenezer A. Oni¹, Temitope Ogunmola², Aminat A. Alowonle³, Damilola A. Omoboyowa¹

5
6 ¹Department of Biochemistry, Adekunle Ajasin University, Akungba-Akoko, Ondo State, Nigeria.

7 ²Pathology, Immunology and Laboratory Medicine, University of Florida, Gainesville, United States

8 ³Department of Chemistry, Obafemi Awolowo University, Ile-Ife, Osun State, Nigeria.

9
10
11
12 **Abstract**

13 **Background:** Despite existing treatments, the prevalence of Type 2 diabetes mellitus (T2D) continues to rise globally,
14 underscoring the need for novel therapeutic strategies. Medicinal plants like *Tinospora cordifolia* have shown potential in
15 traditional medicine for managing various ailments, including diabetes. This study investigates the antidiabetic potential of
16 *T. cordifolia* phytochemicals by targeting dipeptidyl peptidase-4 (DPP-4), a key enzyme in glucose metabolism. **Methods:**
17 A library of 141 bioactive compounds from *T. cordifolia* was compiled and their structures retrieved from PubChem.
18 Ligand preparation was conducted using the Schrödinger Suite, and the crystallographic structure of DPP-4 (PDB ID:
19 2HHA) was prepared for docking. Molecular docking, pharmacophore modeling, MM/GBSA binding energy calculations,
20 and QSAR modeling were performed to assess binding affinities and predict inhibitory activities. Additionally, the QSAR-
21 Toxicity Estimation Software Tool (TEST) was used to evaluate the toxicity profiles of the hit compounds. **Results:**
22 Molecular docking revealed that five *T. cordifolia* compounds exhibited higher binding affinities than the standard drug
23 rosiglitazone, with saponarin showing the highest affinity (-10.40 kcal/mol). MM/GBSA calculations confirmed favorable
24 binding free energies, with saponarin exhibiting a ΔG_{bind} of -44.22 kcal/mol. QSAR modeling predicted that saponarin,
25 astragalín, and tinosinenside had better pIC₅₀ values (5.593 μM , 5.593 μM , and 5.659 μM , respectively) than rosiglitazone
26 (5.059 μM). Pharmacophore modeling identified tinosinenside as having the highest fitness score (0.942). Toxicity
27 assessment indicated that while tinosinenside showed potential for bioaccumulation, other compounds demonstrated
28 moderate toxicity profiles. **Conclusion:** The findings suggest that saponarin, tinosinenside, and astragalín are promising
29 candidates for DPP-4 inhibition and could be developed as novel therapeutic agents for T2D management. Further in vitro
30 and in vivo studies are recommended to validate these computational predictions and explore the clinical potential of these
31 phytochemicals.

32 **Keywords:** *Tinospora cordifolia*, DPP-4 inhibitors, type 2 diabetes, molecular docking, bioinformatics

33
34
35 **Significance:**

36 This study determined *Tinospora cordifolia* phytochemicals as potential DPP-4 inhibitors, offering promising therapeutic
37 candidates for type 2 diabetes.

44

45 Introduction

46 Diabetes mellitus is a metabolic disorder characterized by dysregulation in carbohydrate, fat, and protein metabolism,
47 leading to persistent hyperglycemia due to either insulin deficiency or insulin resistance (Omoboyowa et al., 2023). The
48 disease is classified into type 1 and type 2 diabetes, with type 2 diabetes (T2D) accounting for over 90% of all reported
49 cases, making it a major global health concern (Elekofehinti, 2023). T2D is a chronic condition marked by insulin
50 resistance, resulting in elevated blood glucose levels that require long-term management through lifestyle modifications,
51 dietary control, physical activity, and oral medications (Macalalad et al., 2023). However, there is currently no definitive
52 cure for T2D, and untreated cases can lead to severe complications such as cardiovascular diseases, diabetic retinopathy
53 leading to adult blindness, nephropathy, neuropathy, and lower-limb amputations (Roglic, 2016). The increasing
54 prevalence of T2D worldwide highlights the limitations of existing treatments, underscoring the urgent need for novel
55 therapeutic alternatives to complement current drug regimens.

56 Medicinal plants have played a crucial role in traditional and modern medicine due to their bioactive phytochemicals with
57 therapeutic potential. *Tinospora cordifolia*, commonly known as Guduchi or Giloy, belongs to the Menispermaceae family
58 and has been widely recognized for its pharmacological properties (Dhama et al., 2017). Studies have reported various
59 biological activities of *T. cordifolia*, including anticancer (Singh et al., 2006), antihyperlipidemic (Stanely et al., 2000), and
60 hepatoprotective effects (Bishayi et al., 2002). Additionally, *T. cordifolia* has demonstrated antidiabetic properties in
61 preclinical studies. Rajalakshmi et al. (2009) reported that stem extracts of *T. cordifolia* exhibited antidiabetic effects in
62 streptozotocin-induced diabetic rats, while Sangeetha et al. (2013) highlighted the role of palmatine, a phytoconstituent of
63 *T. cordifolia*, in enhancing glucose uptake via GLUT-4 expression in L6 myotubes. Despite these promising findings, the
64 precise mechanism underlying the antidiabetic action of *T. cordifolia* phytochemicals remains largely unexplored.

65 This study aims to investigate the molecular mechanism by which *T. cordifolia* exerts its antidiabetic effects by targeting
66 key proteins implicated in T2D pathogenesis. One such target is dipeptidyl peptidase-4 (DPP-4), a serine aminopeptidase
67 and transmembrane glycoprotein that plays a crucial role in glucose metabolism (Saini et al., 2023). DPP-4 deactivates
68 incretin hormones, including glucagon-like peptide-1 (GLP-1) and gastric inhibitory peptide, which are essential for
69 stimulating insulin secretion. Inhibiting DPP-4 can prolong incretin activity, thereby enhancing insulin release and
70 improving glycemic control (Macalalad et al., 2023). This study employs advanced bioinformatics approaches, including
71 molecular docking, quantitative structure-activity relationship (QSAR) modeling, pharmacophore modeling, MM/GBSA
72 calculations, and pharmacokinetic profiling, to elucidate the potential of *T. cordifolia* phytochemicals as DPP-4
73 inhibitors. Understanding the molecular interactions between *T. cordifolia* phytochemicals and DPP-4 may pave the way
74 for the development of novel plant-derived therapeutics for T2D management.

75

76

77 Materials and Methods

78 Preparation of Compounds

79 A comprehensive library of 141 bioactive compounds from *Tinospora cordifolia* was compiled through an extensive
80 literature review using Google Scholar and PubChem databases (<https://pubchem.ncbi.nlm.nih.gov/>). The chemical
81 structures of these compounds, along with the co-crystallized ligand and a standard reference drug, were retrieved in
82 Structure Data File (SDF) format. Ligand preparation was conducted using the LigPrep module of Schrödinger Suite
83 (version 2017-V2). The OPLS3 force field was applied at a pH of 7.0 ± 2 , with Epik used for ionization state generation.
84 Desalting and tautomer generation options were enabled to ensure structural integrity. Stereoisomer configurations were
85 maintained to retain specific chiral centers while varying other centers, generating a maximum of one stereoisomer per
86 ligand.

87 Target Protein Preparation and Docking Procedure

88 The crystallographic structure of dipeptidyl peptidase-4 (DPP-4) from *Homo sapiens* (PDB ID: 2HHA) was obtained from
89 the RCSB Protein Data Bank (www.rcsb.org). Monomeric chain A of the protein was prepared using the Protein
90 Preparation Wizard in Schrödinger Suite (version 2017-V2). This process involved adding missing hydrogen atoms,
91 assigning bond orders, optimizing hydrogen-bonding networks, and minimizing energy using the OPLS3 force field. The
92 receptor grid was generated at the binding site of the co-crystallized ligand with coordinates set at $x = 39.15$, $y = 49.23$, and
93 $z = 38.06$ (Omoboyowa, 2024).

94 Prepared *T. cordifolia* compounds were virtually screened against the DPP-4 binding site using the Glide module in
95 Schrödinger Suite. Extra precision (XP) docking mode was employed to ensure high accuracy in binding affinity
96 predictions. The resulting protein-ligand complexes were visualized and analyzed using Discovery Studio Visualizer 2020.
97 The binding interactions and energy profiles were assessed to identify the most promising inhibitors. The crystallographic
98 structure and docking interactions are illustrated in Figure 2.

99 Pharmacophore Modeling and Fitness Score Estimation

100 Pharmacophore modeling was performed using the Receptor-Ligand Pharmacophore Hypothesis module of Schrödinger
101 Suite (version 2017-V2). A pharmacophore hypothesis was generated based on the active site interactions of the
102 crystallographic DPP-4 structure. This hypothesis was then used to screen the *T. cordifolia* compounds. Fitness scores were
103 calculated using the Phase Screen module to evaluate the alignment of the compounds with the pharmacophore features
104 (Omoboyowa, 2022).

105 QSAR Modeling and PIC50 Estimation

106 Experimental datasets of known DPP-4 inhibitors, along with their respective PIC50 values, were retrieved from the
107 ChEMBL database (<https://www.ebi.ac.uk/chembl/>) through BLAST analysis of the DPP-4 FASTA sequence. The datasets
108 were converted into SDF format using DataWarrior software and subsequently imported into the Maestro workspace of
109 Schrödinger Suite. The MacroModel minimization tool was used to optimize the structures. A quantitative structure-
110 activity relationship (QSAR) model was developed based on the experimental PIC50 values. This model was then applied
111 to predict the PIC50 values of the *T. cordifolia* hit compounds to assess their inhibitory potential against DPP-4
112 (Omoboyowa, 2022).

113 Toxicity Prediction Using QSAR-TEST

114 The toxicity of the hit compounds was evaluated using the QSAR-Toxicity Estimation Software Tool (TEST), Version 4.2
115 (Martin, 2016). The primary endpoint analyzed was the oral rat LD50 (lethal dose for 50% of the population). The
116 predicted toxicity values were classified according to the mammalian toxicity scale categories provided by the Agency for
117 Toxic Substances and Disease Registry (ATSDR): Category X (Extreme toxicity), A (Very high toxicity), B (High toxicity),
118 C (Moderate toxicity), and D (Low toxicity) (Sripriya et al., 2019). Additionally, the bioaccumulation factor (BF),
119 developmental toxicity (DT), and mutagenicity of the compounds were assessed using TEST 4.2 to ensure comprehensive
120 safety profiling.

121

122 Results and Discussion

123 The pursuit of novel small molecules that can effectively modulate target protein activity for therapeutic applications is the
124 cornerstone of drug design. Identifying these chemical compounds within the vast chemical space is unattainable without
125 prior knowledge of their molecular structures and interactions (Bodun et al., 2025). Consequently, virtual screening of
126 natural compounds derived from medicinal plants has emerged as a critical method in discovering such bioactive
127 molecules. In this study, bioactive compounds from *Tinospora cordifolia* were screened against dipeptidyl peptidase-4
128 (DPP-4), a significant therapeutic target for type 2 diabetes.

129 Results of Molecular Docking Study

130 Molecular docking, a pivotal tool in drug discovery, employs virtual screening protocols to predict the binding model and
131 affinity of chemical compounds within the binding sites of protein targets (Omoboyowa, 2024). Validation of docking
132 procedures is crucial to ensure the reliability and reproducibility of the protocols. In this study, the co-crystallized ligand
133 from the protein's crystallographic structure was re-docked into its binding domain for superimposition, as illustrated in
134 Figure 2. The root mean square deviation (RMSD) of the superimposed structure was 1.992 Å, falling below the acceptable
135 threshold of 2.0 Å, thereby confirming the protocol's reliability (Balogun et al., 2021).

136 Molecular docking elucidates interactions between small molecules and proteins at the atomic level, highlighting the
137 binding affinity of protein-ligand complexes. Among the 141 natural compounds from *T. cordifolia* screened against DPP-
138 4, five exhibited higher binding affinities than the standard drug, rosiglitazone. Rosiglitazone, a potent member of the
139 thiazolidinedione class, is commonly used alongside other anti-diabetic medications like metformin to enhance the body's
140 insulin sensitivity and regulate blood sugar levels. The results presented in Figure 2 indicate that saponarin demonstrated
141 the highest binding affinity (-10.40 kcal/mol), surpassing the co-crystallized ligand's binding affinity of -9.74 kcal/mol.

142 This superior binding affinity is attributed to the interaction of various functional groups within these compounds and the
143 amino acid residues at the DPP-4 binding site. As depicted in Figure 4, saponarin exhibited the highest number of
144 hydrogen bond interactions among the hit compounds and standards, forming seven hydrogen bonds with ARG 125, GLU
145 205, HIS 126, CYS 551, and ASP 545. Tinosinenside followed closely with six hydrogen bonds involving ARG 669, GLU
146 206, TYR 662, ARG 125, and GLU 205. The co-crystallized ligand formed five hydrogen bonds with ARG 356, ARG 669,
147 ARG 125, and ASN 710. Other hit compounds exhibited fewer hydrogen bonds: astragalin formed four, tyramine one, and
148 higenamine none. Although other interaction types such as salt bridges, pi-sulfur, and carbon-hydrogen bonds were
149 observed (Figure 5), hydrogen bond formation plays a critical role in stabilizing the three-dimensional structure of
150 protein-ligand complexes (Pace et al., 2014).

151 To validate the binding energies of the hit compounds, Molecular Mechanics Generalized Born Surface Area (MM/GBSA)
152 calculations were conducted. MM/GBSA is a widely used method for biomolecular studies, including protein folding,
153 protein-ligand binding, and protein-protein interactions. The binding free energy values (ΔG_{bind}) presented in Figure 3
154 showed that the standard drug (rosiglitazone) and the co-crystallized ligand had the most favorable MM/GBSA scores of -
155 58.25 and -51.79 kcal/mol, respectively. Among the hit compounds, saponarin exhibited the best binding free energy of -
156 44.22 kcal/mol, while tyramine had the least favorable score of -18.06 kcal/mol.

157 **PIC50 Prediction of Hit Compounds via QSAR Modeling**

158 Quantitative Structure-Activity Relationship (QSAR) modeling is a computational technique that establishes correlations
159 between the biological activities of chemical compounds and their structural properties. The principle underpinning QSAR
160 is that variations in structural attributes result in differing biological activities (Kwon et al., 2019). In this study, AutoQSAR
161 modeling of DPP-4 inhibitors retrieved from the ChEMBL database was performed. The dataset was automatically
162 partitioned into 75% training and 25% test sets. The best-performing model, identified as kpls_molprint2D_36, was
163 selected to predict the biological activities of the hit compounds. Model parameters are summarized in Table 2, and the
164 observed versus predicted activities for the training and test sets are illustrated in the scatter plot in Figure 5.

165 Based on predicted activity (pIC50) values, the co-crystallized ligand, with a pIC50 of 6.054 μM , was predicted to be more
166 active than the hit compounds. However, saponarin, astragalin, and tinosinenside, with pIC50 values of 5.593 μM , 5.593
167 μM , and 5.659 μM respectively, demonstrated better predicted activity than the standard drug rosiglitazone, which had a
168 pIC50 of 5.059 μM (Table 3).

169 **Pharmacophore Modeling and Phase Screening of Bioactive Compounds**

170 Pharmacophore modeling is a cutting-edge technology utilized to identify and characterize the potential interactions
171 within ligand-receptor complexes. These interactions encompass steric and electronic features essential for eliciting a
172 biological response (Tyagi et al., 2022). In this study, an E-pharmacophore model was generated to elucidate the steric

173 properties of the co-crystallized ligand critical for optimal interaction with DPP-4. This pharmacophore hypothesis was
174 subsequently applied to screen the hit compounds for shared steric features with the co-crystallized ligand.
175 By comparing these features and evaluating their similarity, fitness scores for the hit compounds and the standard drug
176 were calculated. The pharmacophore hypothesis for the co-crystallized ligand's optimal interaction with DPP-4 comprised
177 four features, as depicted in Figure 6. Fitness scores for the hit compounds are presented in Table 4. Tinosinenside
178 exhibited the highest fitness score of 0.942, with three out of four features matched. The standard drug rosiglitazone
179 followed with a fitness score of 0.564, matching all four features. Astragalín and higenamine matched all four features but
180 had lower fitness scores of 0.476 and 0.433, respectively. Higher fitness scores indicate a stronger predicted biological
181 activity of the compound against the target protein.
182 Overall, the findings from molecular docking, MM/GBSA binding energy calculations, QSAR modeling, and
183 pharmacophore screening provide a comprehensive understanding of the potential anti-diabetic properties of *T. cordifolia*
184 bioactive compounds. The results highlight saponarin, tinosinenside, and astragalín as promising candidates for further
185 investigation and development as therapeutic agents for type 2 diabetes.

186 **Results of the Toxicity Prediction by QSAR-TEST**

187 The toxicity assessment was conducted using the Quantitative Structure-Activity Relationship (QSAR) Toxicity Estimation
188 Software Tool (TEST), a computational model designed to predict the potential toxicity of chemical compounds based on
189 their molecular structure and properties. This tool facilitates the estimation of various toxicity endpoints, including
190 bioaccumulation, developmental toxicity, mutagenicity, and lethal dose (LD50) values.

191 As presented in Table 5, among the screened compounds, *tinosinenside* exhibited a high bio-concentration factor (BCF) of
192 146.22, indicating a greater potential for bioaccumulation in living organisms. In contrast, other small molecules
193 demonstrated moderate bioaccumulation potential, with the exception of *saponarin*, for which the QSAR-TEST tool did
194 not provide a prediction. The bio-concentration factor represents the ratio of a chemical's concentration within an
195 organism to its concentration in the surrounding environment at steady state, serving as a critical indicator of a substance's
196 bioaccumulation potential (Petoumenou et al., 2015). Thus, *tinosinenside* may exhibit slight bioaccumulation in
197 organisms, whereas the other compounds are more likely to be efficiently cleared from biological systems.

198 Developmental toxicity, defined as the potential of a chemical to interfere with the normal development of an organism
199 due to exposure either before conception or during development, was also evaluated (ECHA, 2017). *Higenamine* and
200 *astragalín* were predicted to have developmental toxicity values of 0.76 and 0.58, respectively, classifying them as toxic
201 according to the FDA/TERIS database (Sussman et al., 2003). This suggests that these compounds may pose developmental
202 risks upon exposure.

203 Regarding mutagenicity, only *tyramine* demonstrated a high mutagenicity value of 0.56, indicating a significant potential
204 to cause genetic mutations. Mutagenicity is a crucial factor in assessing the long-term genetic risks posed by chemical
205 compounds.

206 The predicted lethal dose (LD50) values in oral rats, which measure the dose required to cause death in 50% of the test
207 population, revealed that *tinosinenside* exhibited moderate toxicity. In contrast, the remaining compounds, including
208 *saponarin*, *higenamine*, *astragalín*, and *tyramine*, were predicted to have low toxicity levels, indicating a safer profile for
209 potential therapeutic use (Table 5).

210 Overall, the QSAR-TEST predictions provide valuable insights into the safety profiles of the bioactive compounds from *T.*
211 *cordifolia*. While *tinosinenside* shows some bioaccumulation and moderate toxicity, the other compounds demonstrate
212 favorable toxicity profiles, supporting their potential as safer candidates for further investigation in diabetes treatment.

213
214
215

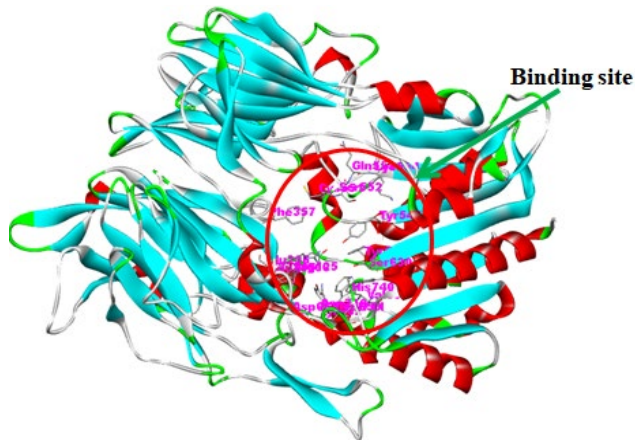
216 **Conclusion**

217 This study demonstrates the potential of *Tinospora cordifolia* phytochemicals as therapeutic agents for type 2 diabetes
218 (T2D) through targeted inhibition of dipeptidyl peptidase-4 (DPP-4). Using advanced bioinformatics approaches,
219 including molecular docking, QSAR modeling, MM/GBSA calculations, and pharmacophore modeling, saponarin,
220 tinosinenside, and astragaloside emerged as promising candidates with superior binding affinities and favorable
221 pharmacokinetic profiles compared to the standard drug rosiglitazone. Saponarin exhibited the highest binding affinity (-
222 10.40 kcal/mol) and demonstrated significant interactions with key amino acid residues in DPP-4. Additionally, toxicity
223 assessments via QSAR-TEST indicated minimal bioaccumulation and acceptable safety profiles for most hit compounds,
224 with tinosinenside showing slight bioaccumulation potential. These findings underscore the promise of *T. cordifolia* in
225 developing novel plant-based therapeutics for T2D management. However, further in vitro and in vivo validation is
226 essential to confirm these bioactivities and ensure clinical applicability.

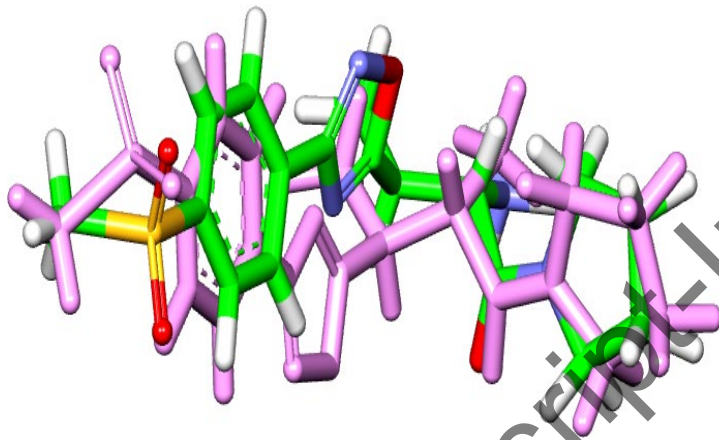
229 **References**

- 230 Balogun, T.A., Iqbal, M.N., Saibu, O.A., Akintubosun, M.O., Lateef, O.M., Nneka, U.C., Abdullateef, O.T. & Omoboyowa,
231 D.A. (2021). Discovery of potential HER2 inhibitors from *Mangifera indica* for the treatment of HER2-Positive breast
232 cancer: an integrated computational approach. *J Biomol Struct Dynam*, 39, 1–12. DOI: [10.1080/07391102.2021.1975570](https://doi.org/10.1080/07391102.2021.1975570)
- 233 Bishayi, B., Roychowdhury, S., Ghosh, S. & Sengupta, M. (2002). Hepatoprotective and immunomodulatory properties of
234 *Tinospora cordifolia* in CCl₄ intoxicated mature albino rats. *J Toxicol Sci*, 27(3),139-46. doi: 10.2131/jts.27.139. PMID:
235 12238138.
- 236 Bodun, D.S., Omoboyowa, D.A., Olofinlade, V.F., Ayodeji, A.O., Mauri, A., Ogbodo, U.C. & Balogun, T.A. (2025). In-
237 silico-based lead optimization of hit compounds targeting mitotic kinesin Eg5 for cancer management. *In Silico*
238 *Pharmacology*, 13,9 <https://doi.org/10.1007/s40203-024-00300-6>
- 239 Dhama, K., Sachan, S., Khandia, R., Munjal, A., Iqbal, H.M.N., Latheef, S.K., Karthik, K., Samad, H.A., Tiwari, R. & Dadar,
240 M. (2017). Medicinal and Beneficial Health Applications of *Tinospora cordifolia* (Guduchi): A Miraculous Herb
241 Countering Various Diseases/Disorders and its Immuno-modulatory Effects. *Recent Pat Endocr Metab Immune Drug*
242 *Discov*, 10(2), 96-111. doi: 10.2174/18722148116666170301105101.
- 243 ECHA (2017). Guidance on information requirements and chemical safety assessment, Version 6.0. Chapter R.7a:
244 Endpoint specific guidance. Helsinki: European Chemicals Agency.
- 245 Elekofehinti, O.O. (2023). Computer-aided identification of bioactive compounds from *Gongronema latifolium* leaf with
246 therapeutic potential against GSK3 β , PTB1B and SGLT2. *Informatics in Medicine Unlocked*, 38, 101202.
247 <https://doi.org/10.1016/j.imu.2023.101202>
- 248 Kwon, S., Bae, H. & Jo, J. (2019) Comprehensive ensemble in QSAR prediction for drug discovery. *BMC Bioinf* 20:521–
249 530. <https://doi.org/10.1186/s12859-019-3135-4>
- 250 Macalalad, M.A.B. & Gonzales, A.A., (2023). In Silico Screening and Identification of Antidiabetic Inhibitors Sourced from
251 Phytochemicals of Philippine Plants against Four Protein Targets of Diabetes (PTP1B, DPP-4, SGLT-2, and FBPase).
252 *Molecules*, 28, 5301. <https://doi.org/10.3390/molecules28145301>
- 253 Martin, T. (2016). User's guide for TEST (version 4.2) (Toxicity Estimation Software Tool): a program to estimate toxicity
254 from molecular structure. EPA/600/R-16/058. Available from: [https://www.epa.gov/chemical-research/toxicity-estimation-](https://www.epa.gov/chemical-research/toxicity-estimation-software-tool-tes)
255 [software-tool-tes](https://www.epa.gov/chemical-research/toxicity-estimation-software-tool-tes)
- 256 Omoboyowa, D. A. (2024). Deciphering phosphodiesterase-5 inhibitors from *Aframemum melegueta*: computational
257 models against erectile dysfunction. *In Silico Pharmacology*, 12, 101. <https://doi.org/10.1007/s40203-024-00284-3>

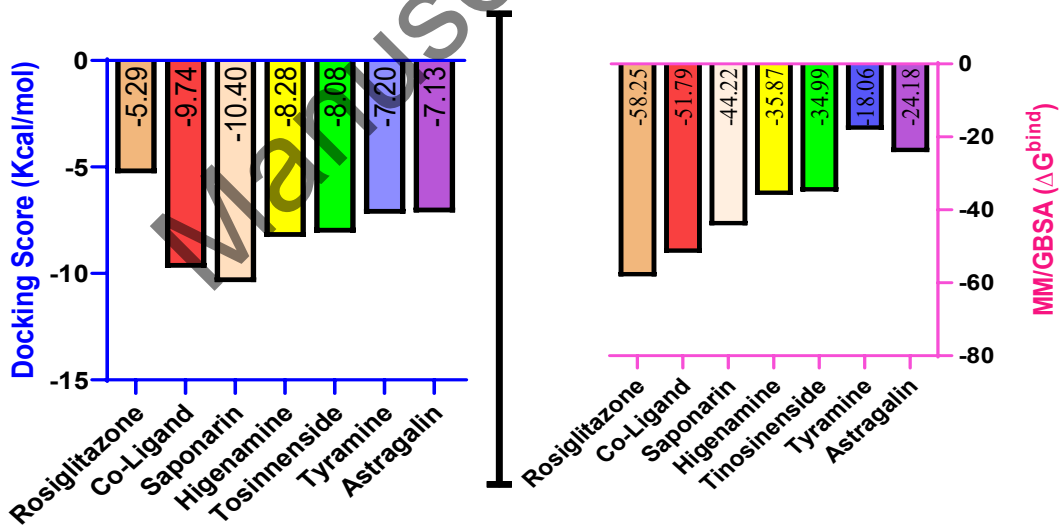
- 258 Omoboyowa, D.A. (2022). Exploring molecular docking with E-pharmacophore and QSAR models to predict potent
259 inhibitors of 14- α -demethylase protease from *Moringa spp.* Pharmacol Res- Modern Chin Med 4,100147.
260 <https://doi.org/10.1016/j.prmcm.2022.100147>
- 261 Omoboyowa, D.A., Agoi, M.D., Shodehinde, S.A., Saibu, O.A., & Saliu, J.A. (2023). Antidiabetes study of Spondias
262 mombin (Linn) stem bark fractions in high-sucrose diet-induced diabetes in *Drosophila melanogaster*. Journal of Taibah
263 University Medical Sciences, 18(4), 663e675. DOI: [10.1016/j.jtumed.2023.01.011](https://doi.org/10.1016/j.jtumed.2023.01.011)
- 264 Pace, C.N., Scholtz, J.M. & Grimsley, G.R. (2014). Forces stabilizing proteins. FEBS Lett., 588(14), 2177-84. doi:
265 [10.1016/j.febslet.2014.05.006](https://doi.org/10.1016/j.febslet.2014.05.006).
- 266 Petoumenou, M.I., Pizzo, F., Cester, J., Fernández, A. & Benfenati, E. (2015). Comparison between bioconcentration factor
267 (BCF) data provided by industry to the European Chemicals Agency (ECHA) and data derived from QSAR models.
268 Environmental Research 142(2015)529–534. DOI: [10.1016/j.envres.2015.08.008](https://doi.org/10.1016/j.envres.2015.08.008)
- 269 Rajalakshmi, M., Eliza, J., Priya, C.E., Nirmala, A.K., & Daisy, P. (2009). Anti-diabetic properties of *Tinospora cordifolia*
270 stem extracts on streptozotocin-induced diabetic rats. African Journal of Pharmacy and Pharmacology, 3, 171-180.
- 271 Roglic, G. (2016). WHO Global Report on Diabetes: A Summary. Int. J. Noncommun. Dis. 1, 3
- 272 Saini, J., Marino, D., Badalov, N., Vugelman, M. & Tenner, S. (2023). Drug-Induced Acute Pancreatitis: An Evidence-
273 Based Classification (Revised). Clin Transl Gastroenterol. 14(8), e00621. doi: [10.14309/ctg.0000000000000621](https://doi.org/10.14309/ctg.0000000000000621).
- 274 Sangeetha, M.K., Priya, C.D. M. and Vasanthi, H.R. (2013). Anti-diabetic property of *Tinospora cordifolia* and its active
275 compound is mediated through the expression of Glut-4 in L6 myotubes, Phytomedicine, 20, 3-4.
276 <https://doi.org/10.1016/j.phymed.2012.11.006>.
- 277 Singh, R.P., Banerjee, S., Kumar, P.V., Raveesha, K.A. & Rao, A.R. (2006). *Tinospora cordifolia* induces enzymes of
278 carcinogen/drug metabolism and antioxidant system, and inhibits lipid peroxidation in mice. Phytomedicine. 13(1-2),74-
279 84. doi: [10.1016/j.phymed.2004.02.013](https://doi.org/10.1016/j.phymed.2004.02.013).
- 280 Sripriya, N., Ranjith, K.M., Ashwin, K.N., Bhuvaneshwari, S. & Udaya, P.N.K. (2019). *In silico* evaluation of multispecies
281 toxicity of natural compounds, Drug and Chemical Toxicology, 44(5), 480-486 DOI: [10.1080/01480545.2019.1614023](https://doi.org/10.1080/01480545.2019.1614023)
- 282 Stanley, P., Prince, M. & Menon, V.P. (2000). Hypoglycemic and other related actions of *Tinospora cordifolia* roots in
283 alloxan induced diabetic rats. J. Ethnopharmacol. 70,9-15. doi: [10.1016/s0378-8741\(99\)00136-1](https://doi.org/10.1016/s0378-8741(99)00136-1).
- 284 Sussman, N.B., Arena, V.C., Yu, S., Mazumdar, S. & Thampatty, B.P. (2003). Decision tree SAR models for developmental
285 toxicity based on an FDA/TERIS database. SAR QSAR Environ Res. 14(2), 83-96. doi: [10.1080/1062936031000073126](https://doi.org/10.1080/1062936031000073126).
- 286 Tyagi, R., Singh, A., Chaudhary, K.K. & Yadav, M.K. (2022). Pharmacophore modeling and its applications, Editor(s): Dev
287 Bukhsh Singh, Rajesh Kumar Pathak, Bioinformatics, Academic Press, Pp: 269-289, <https://doi.org/10.1016/B978-0-323-89775-4.00009-2>.
- 288
289
290
291
292
293



294
295 Figure 1: Crystal structure of DPP-4 (2HHA)
296



297
298 Figure 2: Validation of docking procedure by superimposition of the co-crystallized ligand

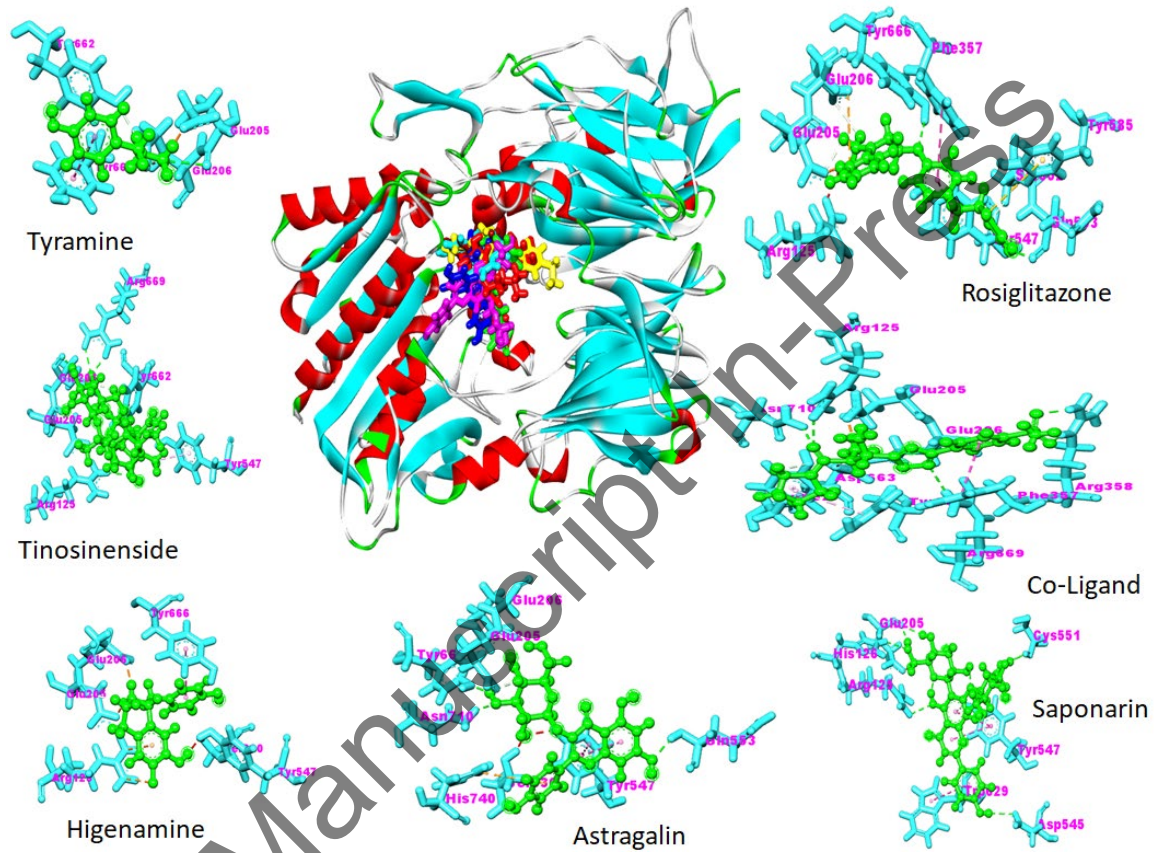


299
300 Figure 3: Representation of the binding affinity and MM/GBSA (ΔG_{bind}) of hit molecules
301

302 Table 1: Binding interactions of hit compounds against target of diabetes

Compounds ID	No of H-bond	Interacting Residues
Rosiglitazone	2	GLN 553; TYR 666
Co-Ligand	5	ARG 356; ARG 669; ARG 125; ASN 710
Saponarin	7	ARG 125; GLU 205; HIS 126; CYS 551; ASP 545
Astragalin	4	ASN 710; TYR 662; GLU 206; GLN 553
Higenamine	NIL	NIL
Tinosinenside	6	ARG 669; GL;U 206; TYR 662; ARG 125; GLU 205
Tyramine	1	GLU 205

303



304

305

Figure 4: Interactions of the hit compounds and amino acid residues at DPP-4 binding site

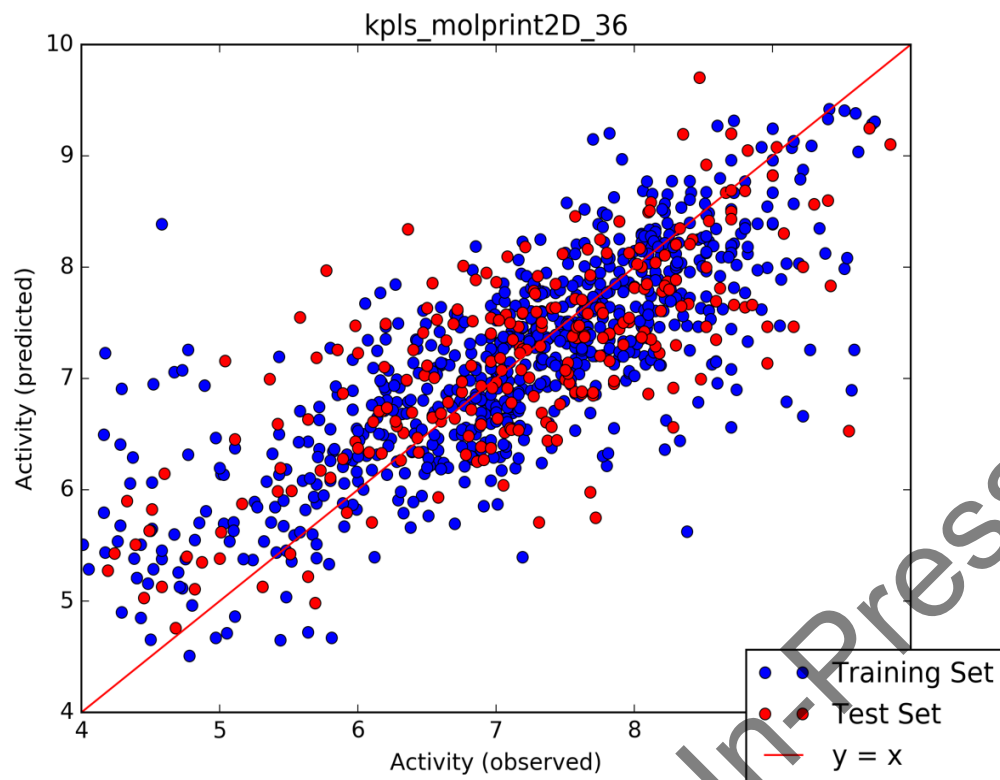
306

307

Table 2: Parameters corresponding to the selected model

Best Model	S.D	R ²	RMSE	Q ²
kpls_molprint2D_36	0.5180	0.7823	0.6136	0.5487

308



309

310 Figure 5: Scatter plot of the observed and predicted activity

311

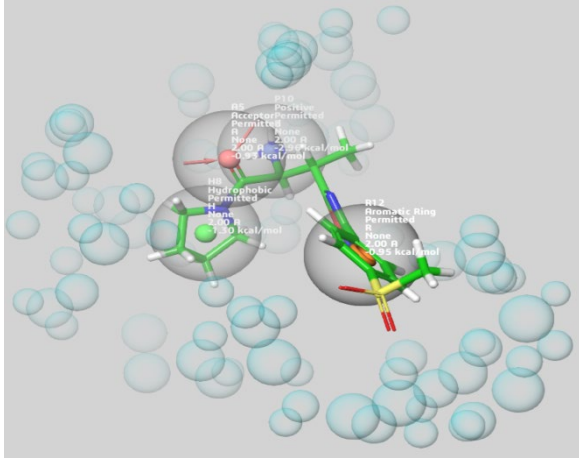
312 Table 3: PIC50 of hit compounds

Compound ID	pIC50 (μm)
Rosiglitazone	5.059
Co-Ligand	6.054
Saponarin	5.593
Astagalin	5.593
Higenamine	5.036
Tinosinenside	5.659
Tyramine	4.863

313

314

315



316
317 **Figure 6: E-pharmacophore hypothesis between co-crystallized ligand and DPP-4**

318
319 **Table 4: Fitness score of hit compounds**

Compound ID	Matched Ligand sites	Fitness score
Rosiglitazone		0.564
Co-Ligand		0.452
Saponarin		0.412
Astragalin		0.476
Higenamine		0.433
Tinosinenside		0.942
Tyramine		0.455

320
321
322 **Table 5: Prediction of toxicity parameters of the hit compounds**

Compound ID	Bio-concentration Factor	Developmental Toxicity		Mutagenicity		Oral Rat	
		Value	Result	Value	Result	LD ₅₀ (mg/kg)	Category
Saponarin	NA	0.40	DNT	0.12	-ve	3433.94	D
Higenamine	9.48	0.76	DT	0.47	-ve	1895.65	D
Tinosinenside	149.22	0.42	DNT	0.08	-ve	33.90	C
Tyramine	2.59	0.44	DNT	0.56	+ve	1170.73	D
Astragalin	13.77	0.58	DT	0.38	-ve	2576.37	D

323 DT: Developmental toxicant; DNT: Developmental Non-toxicant; -ve: Mutagenicity negative; +ve: Mutagenicity positive;
324 NA: Not applicable; C: Moderate toxicity; D: Low toxicity

325